α- PARTICLE INDUCED FUSION - FISSION DYNAMICS

AT E= 140 MeV

A dissertation submitted for partial fulfillment of the requirement for the award of the degree of

Masters of Science
in
PHYSICS

Under the supervision of

Dr. Manoj Sharma

Submitted by

Amanjot Kaur Sahni

Roll no. – 300804001

School of Physics and Materials Science
Thapar University
Patiala – 147004 (PUNJAB) INDIA

Dedicated

to

Hon'ble Prof. Manoj Sharma

CERTIFICATE

This is to certify that Amanjot Kaur Sahni, Roll No. 300804001 has worked on this dissertation as a partial fulfillment for award of the degree of MASTERS OF SCIENCE IN Physics. I certify that the matter embodied in this report is of candidate's own record and not submitted to any other university in any part or full form for the award of such a degree.

Dr. Manoj Sharma
Associate Professor
SPMS, Thapar University
Patiala.

Countersigned By:

Dr. O.P.Pandey
(Prof. & Head)
School of Physics and Materials Science,
Thapar University,
Patiala

Dr. R.K.Sharma
Dean of Academic Affairs
Thapar University,
Patiala.

3

Acknowledgement

I owe my deepest gratitude to Dr. Manoj Sharma, my worthy supervisor Associate Professor SPMS, Thapar University, who has been an inspiration during my research work. Without him, this thesis would not have been possible. I thank him for his patience and encouragement that carried me on through difficult times, and for his insights and suggestions that helped to shape my research skills. I express my sincere thanks to him for his valuable guidance in carrying out work under his effective supervision, encouragement and cooperation. His visionary thoughts have influenced me greatly. His dynamical attitude has empowered me with zeal of energy to conquer the minor details of my research work.

I also thank Dr. O. P. Pandey, Professor and Head, School of Physics and Material Science for his support and providing facilities.

A special word of thanks to Gudveen Sawhney, Research Scholar for the help and valuable suggestions whenever I needed out of her busy schedule.

Special thanks are due to all my friends and the staffs at the School of Physics and Material Sciences for providing me a friendly atmosphere and encouraging me throughout this work.

I am deeply thankful to my Family, their moral support and patience has bared fruit through completion of this Thesis.

Thapar University

Amanjot Kaur Sahni

Roll no. 300804001

Date

ABSTRACT

Alpha particle induced fusion fission dynamics has been studied in present work for four targets i.e. ^{nat}Ag, ^{165}Ho, ^{139}La and ^{197}Au. The dynamical cluster-decay model (DCM) has been used for present set of calculations. The DCM based cross-section find reasonable comparison with experimental data for ^{nat}Ag, ^{139}La, ^{165}Ho and ^{197}Au. In case of ^{139}La, fragments in the fission range are largely suppressed and a cluster type emission is observed. All the calculations are done at incident energy E=140 MeV so the results carry some useful information regarding α-induced fission of nuclei under considerations.

The present work consists of three chapters. The first chapter is introductory in nature. The second chapter consists of dynamical cluster-decay model developed to study the decay of compound nuclei (CN) formed in low-energy reactions. The Dynamical Cluster Decay Model (DCM) is a vibrant model which includes the deformation effects of nuclear systems and the preformation probability (one of the important parameter of DCM) imparts much needed nuclear structure information. The results are summarized in chapter3.

TABLE OF CONTENTS

List of figures

CHAPTER -1

INTRODUCTION

Nuclear physics is a branch of the physics which is concerned with the structure of atomic nuclei, and the understanding of potential ways in order to manipulate atomic nuclei. This branch dates to the early 20th century, when scientists began to realize that the atom had a structure and that understanding this structure could be important. Thus branch of Physics which deals with study of nuclear processes is Nuclear Physics.

Nuclear physics could be said to date from 1896, the year Becquerel observed that photographic plates were being fogged by an unknown radiation emanating from uranium ores. He had accidentally discovered radioactivity, the fact that some nuclei are unstable and decay spontaneously. The name was coined by Marie Curie two years later to distinguish this phenomenon from induced forms of radiation.

Team of Pierre and Marie Curie, Rutherford and his collaborators established that there were two distinct types of radiation involved, named by alpha and beta rays. In 1900 a third type of decay was discovered by Villard that involved the emission of photons, the quanta of electromagnetic radiation. At about the same time, J.J. Thomson suggested a model where the electrons were embedded and free to move in a region of positive charge filling the entire volume of the atom-the so-called 'plum pudding model'. In 1911, Rutherford and his collaborators, Geiger and Marsden yielded most important information about the nucleus. Rutherford showed that positive charge was concentrated in a small region at the centre of atom called nucleus.

To explain the results of these experiments Rutherford formulated a 'planetary' model, where the atom was likened to a planetary system, with the electrons (planets) occupying discrete orbits about a central positively charged nucleus (Sun). Photons of a definite energy would be emitted when electrons moved from one orbit to another, this model explained the discrete nature of the observed electromagnetic spectra when excited atoms decayed. According to classical physics, the electrons in the planetary model would be constantly accelerating and would therefore lose energy by radiation, leading to the collapse of the atom. This problem was solved by Bohr in 1913. He applied the newly emerging quantum theory and the result was the now well-known Bohr model of the atom. Refined modern versions of this model, includes relativistic effects described by the Dirac equation which are capable of explaining various phenomena in Nuclear Physics.

These ideas form the essential framework of our understanding about the nucleus, where the nuclei are bound states of nucleons held together by a strong charge-independent short-range force.

After the discovery in the early 20th century that radioactive elements, such as radium, release immense amounts of energy, according to the principle of mass–energy equivalence, the pursuit of nuclear energy for electricity generation began. But means of harnessing such energy was impractical, because intensely radioactive elements were short-lived. However, the dream of harnessing atomic energy was quite strong, even it was dismissed by fathers of Nuclear physics like Ernest Rutherford as moonshine.

In 1932, James Chadwick demonstrated the existence of an electrically neutral particle of approximately the same mass as the proton. He discovered the neutron, which was immediately recognized as a potential tool for nuclear experimentation because of its neutral electric charge.

Experimentation with bombardment of materials with neutrons led Frédéric and Irène Joliot-Curie to discover induced radioactivity in 1934, which allowed the creation of radium-like elements at much less price than natural radium.

Lise Meitner and Meitner's nephew, Otto Robert Frisch conducted experiments with the products of neutron-bombarded uranium for further investigation. They determined that the relatively tiny neutron split the nucleus of the massive uranium atoms into two roughly equal pieces. This was an extremely surprising result because all other forms of nuclear decay involved only small changes to the mass of the nucleus, whereas this process involved a complete rupture of the nucleus. They named this process as Fission and it was considered as a type of nuclear reaction.

Thus the term fission was first used by the German physicists Lise Meitner and Otto Frisch in 1939 to describe the disintegration of a heavy nucleus into two lighter nuclei of approximately equal size. The conclusion that such an unusual nuclear reaction can in fact occur was the culmination of a truly dramatic episode in the history of science, and it set in motion an extremely intense and productive period of investigation.

In the half century preceding World War II, a number of discoveries were made which in aggregate demonstrated the theoretical possibility of nuclear fission. On December 2, 1942, Enrico Fermi produced the first sustained fission reaction with an experiment performed at the University of Chicago. Fission is a chemical reaction which involves the strong nuclear force, which holds atoms together, and the electro static force which attempts to pull them apart.

Fission describes the process which takes place when a heavy nucleus is caused to break into roughly equal parts, known as fission fragments. A nucleus splits into several smaller fragments. These fragments, or fission products, are about equal to half the original mass. The fission occurs when light particles are used as projectiles on heavy elements and fragments with different masses and energies are obtained. Nuclear processes are used to measure the properties of nuclei. Fission is occurring naturally all around us resulting in the decomposition of heavier elements into lighter ones.

Nuclear fission is a complex process that involves the rearrangement of hundreds of nucleons in single nucleus to produce two separate nuclei. A complete theoretical understanding of this reaction would require a detailed knowledge of the forces involved in the motion of each of the nucleons through the process. Since such knowledge is still not available, it is necessary to construct simplified models of the actual system to simulate its behavior and gain as accurate a description as possible of the steps in the process. The successes and failures of the models in accounting for the various observations of the fission process can provide new insights into the fundamental physics governing the behavior of real nuclei, particularly at the large nuclear deformations encountered in a nucleus undergoing fission.

In order for a nuclear process (reaction) to occur, the nucleons in the incident particle or projectile must interact with the nucleons in the target. Thus the energy must be high enough to overcome the natural electromagnetic repulsion between the protons. This energy barrier is called the Coulomb barrier. If the energy is below the barrier, the nuclei will bounce off each other. Early experiments by Rutherford used low-energy alpha particles from naturally radioactive material to bounce off target atoms and measure the size of the target nuclei. A specific reaction is studied by measuring the angles and kinetic energies of the reaction products. The most important quantity of interest for a specific set of kinematic variables is the reaction cross section.

The following graph shows the potential energy for nuclear fission as a function of the degree of nuclear deformation or the average separation of the two fission fragments. The graph is plotted against r, the separation of two fission fragments. The curve is supposed to be divided into three fragments as shown in Fig. 1.1

In region 1, the fragments are completely separated and their potential energy is simply the electrostatic coulomb energy resulting from the mutual repulsion of two positively charged nuclear fragments.

In Region 2, fragments reach critical distance r_c, where the potential energy curve has a maximum value E_b. This corresponds to barrier height and explains why fission does not take place spontaneously in all cases where $E_f > 0$.

An additional amount of energy $E_a = E_b - E_f$, the activation energy is required by the nuclear system before the potential barrier can be surmounted and fission can take place. In Region 3, the fragments have coalesced and the short range nuclear forces have become predominant.

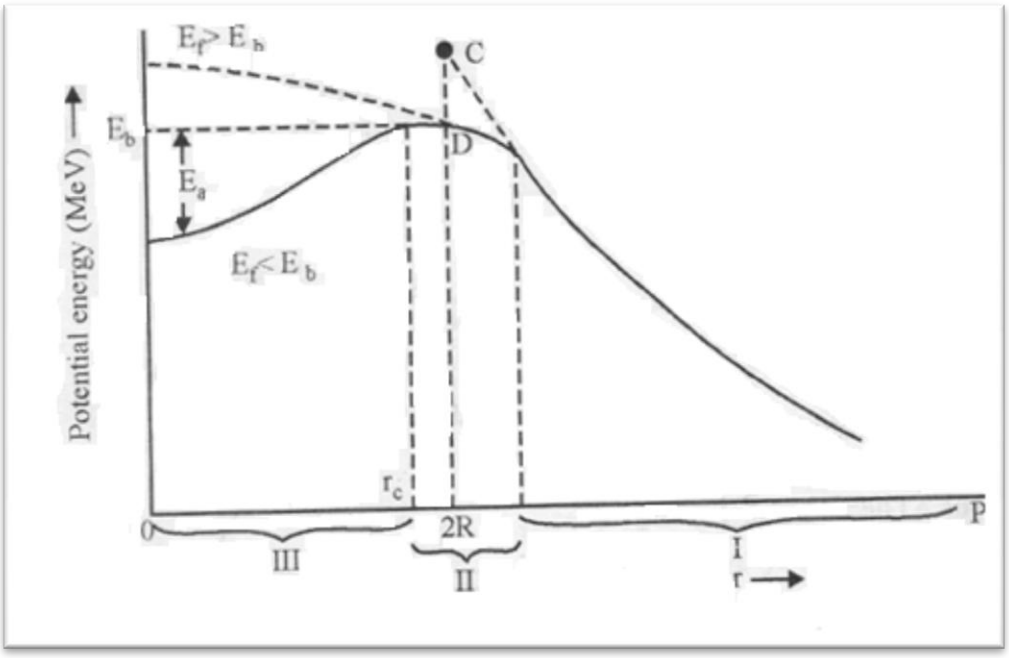

Fig. 1.1 Potential energy curve for fission

TYPES OF NUCLEAR FISSION

INDUCED FISSION

Induced fission – The process in which fission is induced in the target nucleus. Fission can be induced by exciting the nucleus to energy equal to or greater than that of the barrier. This can be done by gamma-ray excitation (photo fission) or through excitation of the nucleus by the capture of a neutron, proton, or other particle such as α particle (particle-induced fission).The height and shape of the fission barrier are dependent on the particular nucleus being considered. The binding energy of a particular nucleon to a nucleus will depend on in addition to the factors considered above, the odd–even character of the nucleus. Although the heavy elements are unstable with respect to fission, the reaction takes place to an appreciable extent only if sufficient energy of activation is available to surmount the fission barrier. The particle used to induce fission strikes the target and compound nucleus is formed which is highly unstable. Compound nucleus splits in two comparable fragments with emission of lighter particles such as neutrons. Huge amount of energy is evolved in induced fission reactions.

U-235 is able to undergo *induced fission*, when a free neutron bombards a U-235 nucleus. Under induced fission, the free neutron will be absorbed by the U-235 nucleus and cause the atom to become unstable and split immediately. The action of capturing the neutron and splitting the atom takes place within a matter of picoseconds.

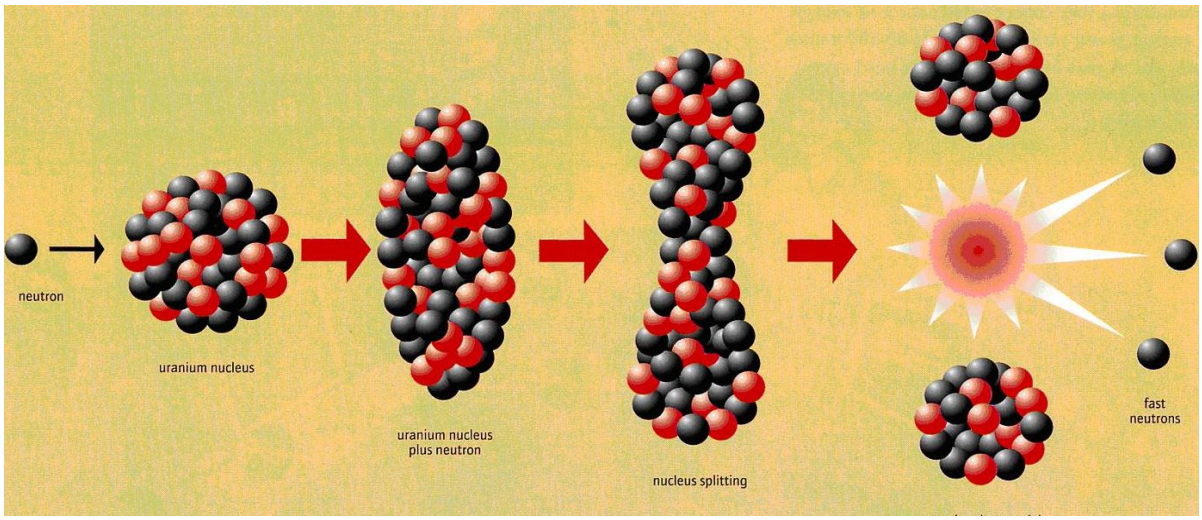

Fig. 1.2 Mechanism of Induced fission

The isotope ^{235}U, with an abundance of only 0.7% in natural uranium, is commonly used to produce electricity in nuclear fission reactors**.** This isotope has the distinctive and useful property of undergoing nuclear fission through interaction with thermal-energy neutrons (neutrons with average speeds of only a few km/s). The other main isotope of uranium, ^{238}U, does not undergo nuclear fission with thermal neutrons, but it does capture neutrons to form the isotope ^{239}Np that then decays to ^{239}Pu. This isotope of plutonium undergoes nuclear fission with thermal neutrons with a higher probability than that of ^{235}U. The energy released in the fission of ^{235}U and ^{239}Pu, mainly in the form of kinetic energy of the fission fragments, provides the heat to run the turbines that generate electricity at a nuclear fission power plant.

SPONTANEOUS FISSION

The spontaneous nuclear fission rate is the probability per second that a given atom will fission spontaneously--that is, without any external intervention. Spontaneous fission is a form of radioactive decay characteristic of very heavy isotopes. It was discovered (1941) by the Russian physicists G.N. Flerov and K.A. Petrzhak in uranium-238, is observable in many nuclear species of mass number 230 or more. The spontaneous fission was identified by their observations of uranium in the Moscow Metro Dinamo station, 60 meters' (200 ft) deep underground. It is theoretically possible for any atomic nucleus whose mass is greater than or equal to 100 atomic mass units (u), i.e. elements near ruthenium. In practice, however, spontaneous fission is only energetically feasible for atomic masses above 230 u (elements near thorium). The elements most susceptible to spontaneous fission are the high-atomic-number actinide elements, such as mendelevium and lawrencium, and the trans-actinide elements, such as Rutherfordium. The nuclei of atoms of these elements are naturally unstable, and they can just split by themselves. The instability is a characteristic of these and some other elements, and this is because these large nuclei are so massive that their nuclear binding energy cannot hold them together indefinitely. The unstable nucleus just falls or breaks apart by itself. The nucleus splits in two parts of approximately the same size, and these are the *fission fragments* from the decay event. One or more neutrons will be released at this time, too. The fission fragments recoil with a great deal of kinetic energy. The below given figure 1.3 describes spontaneous fission.

Fig. 1.3

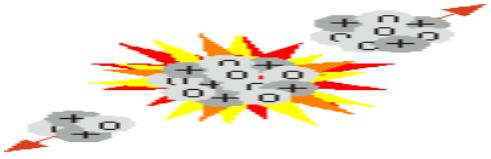

For uranium and thorium, the spontaneous fission mode of decay does occur, but it is not seen for the majority of radioactive breakdowns, and it is usually neglected except for the exact considerations of branching ratios when determining the activity of a sample containing these elements. Mathematically, the criterion for whether spontaneous fission can occur is approximately:

$$Z^2/A \geq 45.$$

Where Z is the atomic number and A is the mass number

As the name suggests, spontaneous fission gives the same result as induced nuclear fission. However, like other forms of radioactive decay, it occurs due to quantum tunnelling, without the atom having been struck by a neutron or other particle as in induced nuclear fission. Spontaneous fissions release neutrons as all fissions do, so if a critical mass is present, a spontaneous fission can initiate a chain reaction. The neutrons may then be used to inspect airline luggage for hidden explosives, to gauge the moisture content of soil in the road construction and building industries, to measure the moisture of materials stored in silos, and in other applications.

LITERATURE SURVEY

Nuclear fission has been an extensively studied field of nuclear physics for a long time .It has been found from the literatures that research/work on particle induced fission (proton, neutron or alpha particle) is being studied since last 60 years. Particle induced fission studies are carried out at different laboratories for different aims. The study differs from other because of different energies of incident particles involved in the nuclear reactions. These types of mechanisms are studied for measurement of cross sections, fission probability, mass distribution and fragment masses for different target nuclei.

Fission dynamics provides an invaluable testing ground for nuclear many-body theory. Many of the crucial questions arising in heavy-ion reactions concerning dissipation mechanisms, the validity of fluid-dynamic and mean-field approximations are relevant to fission. Availability of comprehensive, systematic fission data and the reasonably well developed state of computational technology, it is worthwhile to attempt to use fission as a definitive test of alternative theoretical approaches.

In the 1950s, when alpha particle beams up to 50 MeV became available at the Crocker Laboratory in Berkeley, the Seaborg research group Ref. [1] carried out a number of experimental studies of fissionability of nuclides in the Th-Pu mass region. These involved the measurement of production cross sections of the fragments produced in competition with fission .At the time , the state of knowledge of the mechanisms involved in the interaction of alpha particles with heavy nuclides precluded any calculation of the fissionability of a given nuclide at given excitation energy.

At nearly the same time, Gadioli et *al*. Ref [2] made use of exciton model for proton induced reactions. Somewhat later, the exciton model was extended Ref. [3] to consider alpha induced reactions on non fissile nuclei. This work was greatly enhanced by the then newly available data on breakup mechanisms in alpha nucleus reactions performed largely Holmgren, Chang, and co workers Ref [4-6] at Maryland. This extended model was, known as OMEGA Ref [3].

There follows a discussion of the OMEGA Model, in particular as it is affected by the evolution of the relative contributions of various alpha-nucleus interaction modes, a description of the calculations performed, and a comparison of the theoretical predictions with the experimental data. On nine target nuclei α particle of energies from 20-50 MeV have been considered.

Study of the fission process has been utilized for the understanding of the existence of the two types of mass distributions, symmetric and asymmetric, and the competition between them. Measurements of mass and energy distributions in fission have been made by a large number of experimenters for many different fissioning nuclei over a large range of excitation energies.

Experiment performed by H.C.Britt et *al*. Ref. [7] under the auspices of the U. S. Atomic Energy Commission (1963) yielded information on the mass distributions and the details of the kinetic energy release from a series of charged particle-induced fission reactions. The fissioning compound nuclei range from thallium for which the mass distributions are symmetric, to plutonium for which the fission is predominantly asymmetric.

Absolute cross sections for proton induced fission of Uranium isotopes have been calculated by J. R. Boyce et *al* Ref. [8]. Cross sections are measured for ^{233}U, ^{234}U, ^{235}U, ^{236}U and ^{238}U at proton energies ranging from *5.0* to 30.0 MeV. The experiments were performed at Triangle Universities Nuclear Laboratory (TUNL). Cross section data for a series of targets of adjacent mass number and for an extended energy range permit an attempt to unfold the individual contributions of the multiple chance fission process occurring in the measurement.

Alpha induced fission is carried out by T. Datta et *al*. Ref. [9] to study angular distribution in fission products having ^{232}Th and ^{238}U as the fissioning systems as a function of mass asymmetry. The angular distribution of fission products or heavy-ion reaction products is investigated with multiple objectives. In low- and medium-energy fission a major objective of such investigations has been the understanding of the properties of the fissioning nucleus. The fission fragment angular distribution is determined at the second saddle point due to the tilting mode of rotation. Angular anisotropies of fission products are determined as a function of mass asymmetry in 29 MeV alpha-induced fission of ^{238}U and 39 MeV alpha particle induced fission of ^{238}U and ^{232}Th. The anisotropy is seen to increase with the alpha energies in both the fissioning systems. The increase in the anisotropy with the energy is seen to be more in ^{232}Th as compared to that in the ^{238}U system.

Since the discovery of fission and the first theoretical description of the mechanism, much has been learned about the fission process and its observables. Both fundamental and applied interests have driven a thorough study of fission of actinides induced by low-energy charged particles. Throughout the years several proton-induced fission experiments have been carried out at energies above 20 MeV. Most of them concern fission of actinides, i.e., Thorium and Uranium. Many of the measurements on Thorium have been performed at incident energies

below 100 MeV. Proton-induced fission at 190 MeV of ^{nat}W, ^{197}Au, ^{nat}Pb, ^{208}Pb, and ^{232}Th is studied by M.C. Duijvestijn et *al.*Ref. [10].

Fission cross sections and mass yield curves are calculated with the intranuclear cascade code for fission. For ^{nat}W, ^{197}Au, ^{208}Pb, and ^{nat}Pb the fission process results in a symmetric mass distribution. In the case of ^{232}Th the mass yield curve is decomposed into a mixed symmetric-asymmetric contribution originating from fissioning nuclides in the neighborhood of the target mass and a purely symmetric contribution from very neutron-deficient nuclides.

PRESENT WORK

The binary fission process in heavy elements has been systematically studied with energetic probes such as photons, protons, α particle, as well as with heavy ions. The details of such experiments can be found in Refs. [11] and [12]. Less is known about the fission of lighter nuclei and higher energies where such nuclei can fission. If the angular momentum is high then the fission barrier is reduced and even light systems like ^{60}Zn can undergo fission [13]. Here we will concentrate on reactions induced by light charged particles and in particular alpha (α) particle.

In the present work binary fission induced by 140 MeV α particles has been studied for ^{nat}Ag , ^{139}La, ^{165}Ho, and ^{197}Au targets Ref [14]. The measured quantities are the total kinetic energies, fragment masses, and fission cross sections. The DCM results are compared with experimental data and other systematics. The DCM cross sections find nice comparison with experimental data for ^{nat}Ag, ^{165}Ho, and ^{197}Au targets where as the fission fragments in case of α- induced fission on ^{139}La targets we observe that fragments in the fission range are largely suppressed and a cluster type of emission is observed.

REFERENCES

[1] R. A. Glass, R. J. Carr, J. W. Cobble, and G. T. Seaborg, Phys. Rev. **104,** 434 (1956).

[2] J. J. Hogan, E. Gadioli, E. Gadioli-Erba, and C. Chung, Phys. Rev. C 20, 1831 (1979).

[3] E. Gadioli, E. Gadioli-Erba, J. J. Hogan, and B. V. Jacak, Phys. Rev. C 29, 76 (1984).

[4] R. W. Koontz, C. C. Chang, H. D. Holmgren, and J. R. Wu, Phys. Rev. Lett. **43,** 1862 (1979).

[5] J. R. Wu, C. C. Chang, H. D. Holmgren, and R. W. Koontz, Phys. Rev. C **20,** 1284 (1977).

[6] H. D. Holmgren, C. C. Chang, R. W. Koontz, and J. R. Wu, in *Proceedings of the 2nd International Conference on Nuclear Reaction Mechanisms, Varenna, 1979,* edited by E. Gadioli (CLUED, Milan, 1979), p. 35.

[7] H. C. BRITT**,** H. E. WEGNER, AND JUDITH C. GURSEY, Phys.Rev.**129,** 5(1963)

[8] J. R. Boyce, T. D. Hayward, R. Bass, H. W. Newson, E.G. Bilpuch, and F. O. Purser, Phys. Rev.C10,1(1974)

[9] T. Datta, S. P. Dange, H. Naik, and S. B. Manohar, *Bhabha Atomic Research Centre,Bombay*Phys.Rev.C48,1(1993)

[10] M. C. Duijvestijn and A. J. Koning *Netherlands Energy Research Foundation* J. P. M. Beijers, A. Ferrari, M. Gastal, J. van Klinken, and R. W. Ostendorf *Kernfysisch Versneller Instituut KVI (The Netherlands) Phys. Rev. C 59,2(1999)*

[11] R.Vandenboosch and J.R.Huizenga, Nuclear Fission (Academic Press, New York/London, 1973).

[12] C. Wagemans, The Nuclear Fission Process (CRC Press, Boca Raton, 1991).

[13] W. von Oertzen et al., Phys. Rev. C 78, 044615 (2008).

[14] A. Buttkewitz,H. H. Duhm, F. Goldenbaum, H. Machner,, and W. Strauß Phy Rev C **80**, 037603 (2009)

CHAPTER -2

DYNAMICAL CLUSTER DECAY MODEL

The dynamical cluster-decay model (DCM) is developed for the decay of hot and rotating compound nuclei (CN) formed in low-energy heavy-ion reactions. The model is a non-statistical description for the decay of a compound nucleus (CN) to light particles, intermediate mass fragments, fusion-fission and quasi-fission (equivalently, capture) processes, and hence is given as an alternative to the well known Hauser-Feshbach analysis (statistical evaporation code) and statistical fission models. The quasi-fission or capture is the non-CN contribution, determined empirically. The deformations and orientation degrees of freedom (for compact orientations) of the incoming nuclei and of out-going nuclei/fragments are also included. The model considers all decay products as dynamical mass motions of preformed fragments or clusters through the interaction barrier, thereby including structure effects of the CN explicitly.

The model is worked out in terms of only one parameter, namely the neck-length parameter, which is related to the total kinetic energy *TKE* (T) or effective *Q* value $Q_{\rm eff}(T)$ at temperature *T* of the hot CN and is defined in terms of the CN binding energy and ground-state binding energies of the emitted fragments. The emission of both the light particles (LP), with $A \leq 4$, $Z \leq 2$, as well as the complex intermediate mass fragments (IMF), with $4 < A < 20$, $Z > 2$, is considered as the dynamical collective mass motion of preformed clusters through the barrier. Within the same dynamical model treatment, the LPs are shown to have different characteristics compared to those of the IMFs. The systematic variations of the LP emission cross section ($\sigma_{\rm LP}$) and IMF emission cross section ($\sigma_{\rm IMF}$) calculated from the present DCM match exactly the statistical fission model predictions. A non statistical dynamical description is developed for the first time for emission of light particles from hot and rotating CN.

2.1 INTRODUCTION

A comprehensive study of various types of emission from the ground state as well as excited states of compound nucleus (CN) formed in low energy reaction is important, as it gives information about the nuclear structure aside the underlying nuclear forces .At low energies and average nuclear force field acts between decaying fragments which in turn ensures possibility of more than one decay path .This average nuclear force field is largely influenced by entrance channel, angular momentum and the temperature consideration along with contribution of deformed and orientation effects. An extensive study of these nuclear properties lead to a better understanding of reaction dynamics of rare nuclear species that make the unexplored part of the nuclear chart, called exotic nuclei.

The main aim of the work is to study fission dynamics especially the decay of excited compound nucleus using the dynamical cluster decay model (DCM) [1]-[9].It is important to note that deformation and orientation effects of the reaction partner and decay products are explicitly included along with temperature and angular momentum contribution in this model. The ground state cluster decay of radioactive nuclei has also been undertaken with in the preformed cluster decay model [10]-[18].Again having deformation and orientation effects of the cluster as well as daughter nuclei included in it. Details of DCM are given in the section 2.2

This model is a two step model, where the first step is quantum mechanical preformation probability P_0 of the decay products or cluster formed in the mother nuclei and the second step is the penetration of the fragments/ clusters through the interaction barrier. The Preformation Probability (P_0) based on Quantum Mechanical Fragmentation Theory is also discussed here in section 2.4. Penetration probability (P) is given in section 2.5. These two crucial parameters (P_0 and P) have been developed and used [9], [17], 18] to incorporate the deformation effects of oriented nuclei. The assault frequency, υ_0 with which the preformed cluster tries to tunnel the barrier in the ground state decay is discussed in section 2.6.

2.2 The Dynamical Cluster Decay Model (DCM) For Hot and Rotating Compound Nucleus

The dynamical cluster decay model (DCM) [1]-[9] for hot and rotating nuclei (i.e. angular momentum and temperature both not equal to zero) is a reformation of the preformed cluster model of Gupta and collaborators for ground state decay (ℓ =0,t=0)in cluster radioactive (CR)and related phenomena [10]-[18] .like PCM, DCM is also based upon the dynamical (or quantum mechanical) fragmentation theory of cold phenomena in fission dynamics .In DCM, besides the temperature and angular momentum effects in the decay of excited compound nuclei ,the deformation and orientation effect of the decay products are also taken care, especially in the decay of heavy excited CN for which the deformation of the decay product seems to play significant role. The DCM, worked out in terms of the collective coordinates of mass asymmetry $\eta=\frac{A_1 - A_2}{A_1 + A_2}$ and relative separation R respectively gives

(i). The nucleon-division (or exchange)between the outgoing fragments ,and

(ii). The transfer of kinetic energy of incident channel (E_{cm}) to internal excitation (total excitation or total kinetic energy, TXE or TKE) of the outgoing channel. It may be noted that the fixed decay point R = R_a (defined later),at which the process is calculated depends upon temperature T as well as on η (i.e. R(T, η)) .This energy transfer process can be calculated as follows with the help of Fig 2.1

$$E^*_* = E_{c.m} + Q_{in} = IQ_{out}I + TKE(T) + TXE(T) \quad (2.1)$$

The CN excitation E^*_{CN} is related to temperature T (in MeV) and is given by $E^*_{CN} = \frac{1}{9}AT^2 - T(Mev)$.

Using the decoupled approximation to R and η–motions, the DCM defines the decay cross section, in terms of partial waves, as [3]-[9];

$$k= \sqrt{\frac{(2\mu Ec.m)}{h^2}}; \sigma = \sum_{l=0}^{lc} \sigma l = \frac{\pi}{k^2}\sum_{l=0}^{lc}(2l+1)PoP \quad (2.2)$$

Where $P_{o,}$ the preformation probability refers to η-motion and P, penetrability to the R- motion, discussed in section 2.4 and 2.5 respectively. Here the complex fragments (both light and heavy fragments) are treated as the dynamical collective mass motion of preformed cluster or fragments through the barrier .The structure information of the CN enters the model via preformation probability P_o (also known as spectroscopic factor) of the fragments given by the solution of stationary Schrödinger equation in η at the fixed $R=R_{a,}$ the first turning point of the penetrability path shown in figure 2.1 for the different ℓ -values.

$$\left\{-\frac{\hbar^2}{2\sqrt{B_{\eta\eta}}}\frac{\partial}{\partial\eta}\frac{1}{\sqrt{B_{\eta\eta}}}\frac{\partial}{\partial\eta}+V_R(\eta,T)\right\}\psi^{\nu}(\eta)=E^{\nu}\psi^{\nu}(\eta) \tag{2.3}$$

with ν =0,1,2,3,….referring to the ground state and excited state solution .For the decay of the hot compound nucleus, we use the postulate of first turning point

$$R_a=R_t+\Delta R\ (T) \tag{2.4}$$

Where

$$R_t = R_1+R_2 \tag{2.5}$$

ΔR(T) is the neck length parameter that assimilates the neck formation effects .This method is introducing a neck length parameter similar to that used in scission point [21] and saddle point [22],[23]statistical fission model. The R_i are radius vectors which are also made temperature dependent can be calculated as

$$R_i(\alpha_i)=R_{0i}\left[1+\sum_{\lambda}\beta_{\lambda i}Y_{\lambda}^{(0)}(\alpha_i)\right] \tag{2.6}$$

With

$$R_{0i}\ (T) = 1.28A_i^{1/3} - 0.76 + 0.8A_i^{-1/3}\times (1 + 0.0007T^2), \tag{2.7}$$

The corresponding potential V (R_a) acts like an effective Q-value, Q_{eff} , for the decay of the hot CN at temperature T, to two exit-channel fragments observed is, (T=0), defined by

$$Q_{eff}\ (T) = B(T) - [\ B_L(T = 0) + B_H(T = 0)]$$

$$= TKE\ (T) = V\ (R_a\ (T)) \tag{2.8}$$

With B's, as the respective binding energies. The above defined decay of a hot CN into two cold (T=0) fragments, via Eq. (2.8), could apparently be achieved only by emitting some light particle (s)(LPs), like n, p, α, or γ-rays of energy.

By defining Q_{eff} (T) as in Eq. (2.8), in this model we treat the LP emission at par with the heavy fragments, called intermediate mass fragments (IMFs) emission. Thus, in this model a non-statistical dynamical treatment is attempted for not only the emission of IMFs but also of multiple LPs, understood so-far only as the statistically evaporated particles in a CN emission. It may be reminded here that the statistical model (CN emission) interpretation of IMFs is not as good as it is for the LP production [21–26].

In terms of Q_{eff} (T), the second turning R_b satisfies (see Fig. 2.1)

$$V(R_a, l) = V(R_b, l) = Q_{eff}(T, l) = TKE(T). \quad (2.9)$$

with the l -dependence of R_a defined by

$$V(\mathrm{Ra}, l) = Q_{eff}(T, l = 0), \quad (2.10)$$

which means that the R_a, given by Eq. (2.4), is the same for all l -values, and that V (Ra, l) acts like an effective Q-value, Q_{eff} (T, l), given by the total kinetic energy TKE(T). Then, using (2.9), $R_b(l)$ is given by the l -dependent scattering potentials, at fixed T as

$$V(R, T, l) = V_c(Z_i, \beta_{\lambda i}, \theta_i, T) + V_p(A_i, \beta_{\lambda i}, \theta_i, T) + V_l(R, A_i, \beta_{\lambda i}, \theta_i, T) \quad (2.11)$$

Which is normalized to the exit channel binding energy $B_L(T) + B_H(T)$. Such a potential is illustrated in Fig. 2.1, $^{4}He + {}^{108}Ag \rightarrow {}^{112}In$, at ℓ =0 value. The second turning point R_b is marked for the $\ell = 0\hbar$ case of $R_a = R_t + \Delta R(T)$. The decay path for the l -values begins at $R = R_a$.

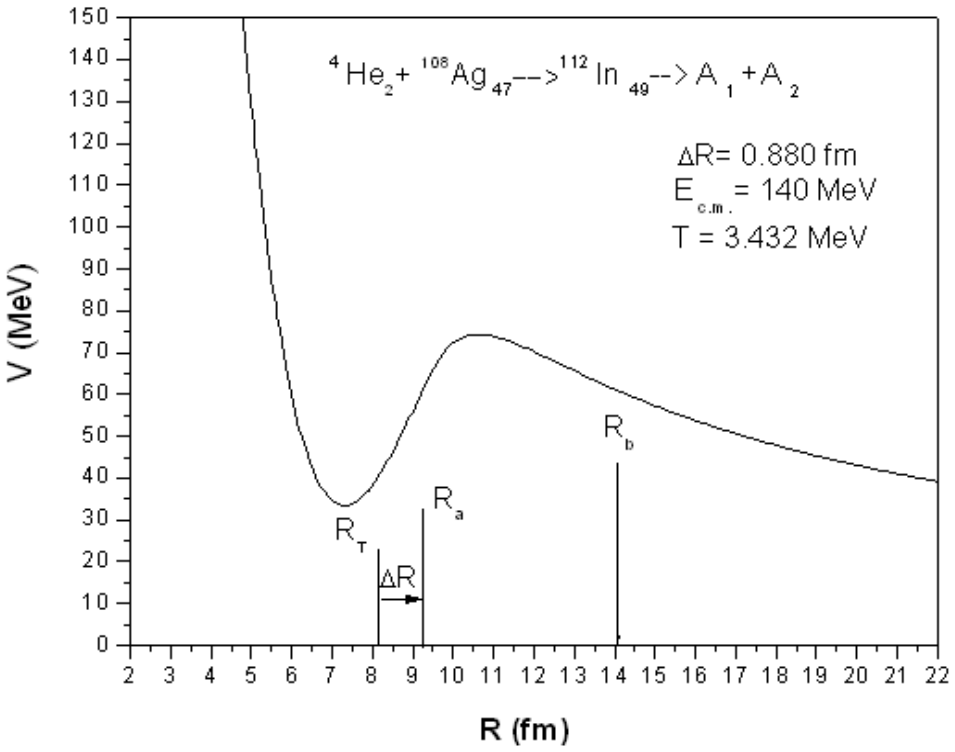

Fig.2.1. Scattering Plot for $^4He_2 + {}^{108}Ag_{47} \rightarrow {}^{112}In_{49}$ reaction

The collective fragmentation potential V(R,η,T) in Eq. (2.11) is calculated according to the Strutinsky method by using the T-dependent liquid drop model energy V_{LDM} of [27], with its constants at T=0 re-fitted [3, 4] to give the recent experimental binding energies given by [42], and again refitted [9] to give the recent experimental binding energies[29] and calculate binding energies[30] (only for those nuclides for which experimental data is not available. the "empirical" shell corrections δU are of Ref. [31] (In the Appendix of [3] and Eq. (8) of [4], a_a=0.5, instead of unity). Then, including the T-dependence also in Coulomb, nuclear proximity, and l -dependent potential in complete sticking limit of moment of inertia, we get

$$V(R,\eta,T) = \sum_{i=1}^{2}[V_{LDM}(A_i, Z_i, T) + \sum_{i=1}^{2}[\delta U_i] exp\left(\frac{-T^2}{T_0^2}\right) + V_c(Z_i, \beta_{\lambda i}, \theta_i, T) + V_P(A_i, \beta_{\lambda i}, \theta_i, T) + V_l(R, \beta_{\lambda i}, \theta_i, T) \quad (2.12)$$

Where the T-dependent terms V_c, V_P and V_l are defined below.

The additional potential due to attractive forces is called the nuclear proximity potential.

For hot deformed nuclei proximity potential [19], [20] is given as;

–

$$V_p(A_i, \beta_{\lambda i}, \theta i, T) = 4\pi R\,(T)\gamma b(T)\Phi(s_0(T)) \qquad (2.13)$$

And, the Coulomb Potential, the potential which describes the force of repulsion between two interacting nuclei due to their charges, acts along the line joining the two nuclei. The Coulomb potential for two interacting spherical nuclei is given as;

$$V_c\left(Z_i, \beta_{\lambda i}, \theta_i, T\right) = \frac{Z_1 Z_2 e^2}{R(T)} + 3Z_1 Z_2 e^2 \sum_{i,i=1,2} \frac{R_i^{\lambda}(\alpha_i,T)}{(2\lambda+1)R(T)^{\lambda+1}}$$
$$Y_{\lambda}^{(0)}(\theta_i)\left[\beta_{\lambda i} + \beta_{\lambda i}^2 Y_{\lambda}^{(0)}(\theta_i)\right] \qquad (2.14)$$

With the radius vector given by Eq. (2.6) and surface thickness parameter

$$b\,(T) = 0.99(1 + 0.009T^2). \qquad (2.15)$$

The rotational motion gives an additional energy due to the angular momentum, known as angular momentum potential which is given as;

$$V_l\,(R, A_i, \beta_{\lambda i}, \theta_i, T) = \frac{\hbar^2\, l\,(l+1)}{2I_s(T)} \qquad (2.16)$$

With the moment-of-inertia,

$$I_s\,(T) = \mu R^2 + \frac{2}{5}A_1 m R_1^{\,2}\,(\alpha_1, T) + \frac{2}{5}A_2 m R_2^{\,2}\,(\alpha_2, T).$$

Further, in Eq. (2.12), within the Strutinsky renormalization procedure, we have defined the binding energy B of a nucleus at temperature T as the sum of liquid drop energy V_{LDM} (T) and shell correction δU (T) i.e.

$$B(T) = V_{LDM}(T) + \delta U \exp(\frac{-T^2}{T_0^2}) \quad (2.17)$$

The T dependent liquid drop part of the binding energy VLDM(T) is from Davidson et al. [27], based on the semi-empirical mass formula of Seeger [32]. For the shell correction δU in Eq. (2.17), since there is no microscopic shell model known that gives the shell corrections for light nuclei, we use the empirical formula of Myers and Swiatecki [31].

The mass parameters $B_{\eta\eta}$ (η), representing the kinetic energy part in Eq. (2.3), are the smooth classical hydro-dynamical masses [33]. Hydrodynamical mass parameter is given in the section - 2.3 for $\upsilon_1 = \upsilon_2 = 0^0$ and R_i taken as temperature dependent.

Finally, the l_c-value in Eq. (2.6) is the critical l-value, in terms of the bombarding energy $E_{c.m}$. The reduced mass μ and the first turning point R_a of the entrance channel η_{in}, given by

$$l_c = R_a\sqrt{(2\mu\,[E_{c.m.} - V\,(R_a, \eta_{in}, l = 0)])}/\hbar \quad (2.18)$$

Or, alternatively, it could be fixed for the vanishing of fusion barrier of the incoming channel, called l_{fus}, or else the l-value (l_{max}) where the light-particle cross-section $\sigma_{LP} \rightarrow 0$. This, however, could also be taken as a variable parameter [22, 34].

2.3 Classical Hydrodynamical Mass Parameters

The kinetic energy part of the Hamiltonian in the equation below enters through the mass parameters.

$$\left[\frac{-\hbar^2}{2\sqrt{B_{\eta\eta}}}\frac{\partial}{\partial_\eta}\frac{1}{\sqrt{B_{\eta\eta}}}\frac{\partial}{\partial_\eta} + V(\eta)\right]\Psi^{\upsilon}(\eta) = E_\eta^{\upsilon}\Psi^{\upsilon}(\eta)$$

We use here the classical mass parameters of Kroger and Scheid [33]. The model of Kroger and Scheid is based on the hydrodynamical flow, as shown in Fig. 2.2. This model gives a simple

analytical expression, whose predictions are shown to compare nicely with the microscopic cranking model calculations. For the Bηη mass we get

$$B\eta\eta = \frac{AmR2}{4}\left[\frac{vt(1+\gamma)}{vc\,1+\left(\frac{vt(1+\gamma)}{vc\,(1+\_\delta 2)}\right)} - 1\right] \qquad (2.19)$$

With

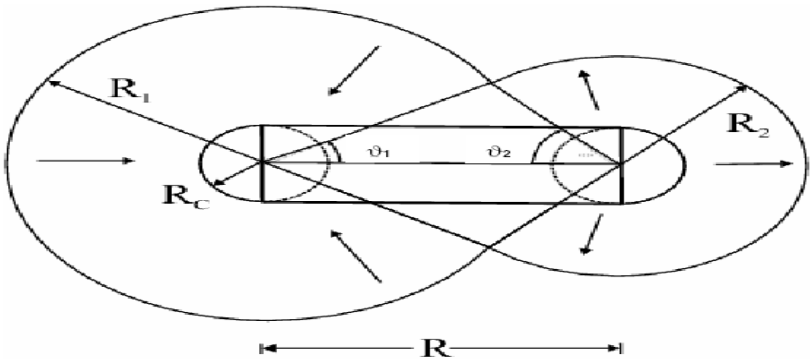

Fig.2.2. The geometry of classical hydrodynamical model for calculating mass parameter $B_{\eta\eta}$

$$\gamma = = \frac{Rc}{2R}\left[\frac{1}{1+\cos\,\upsilon 1}\left(1-\frac{Rc}{R1}\right)+\frac{1}{1+\cos\,\upsilon\,2}\left(1-\frac{Rc}{R2}\right)\right] \qquad (2.20)$$

$$\delta = \frac{1}{2R}[(1-\cos\upsilon_1\,)+(\,1-\cos\,\upsilon 2)] \qquad (2.21)$$

$$v_c = \pi^2 R^2{}_c R \qquad (2.22)$$

And $v_t = v_1+v_2$, is the total conserved volume. The angles υ_1 and υ_2 and geometry of the model are shown in Fig. 2.3. For $\upsilon_1 = \upsilon_2 = 0$, $\delta = 0$ which corresponds to two touching spheres. R_c (is not equal to 0) is the radius of a cylinder of length R, having a homogeneous flow in it; whose existence is assumed for the mass transfer between the two spherical fragments. We have generalized this formalism for deformed nuclei by using the radii R1 and R2 for deformed nuclei, given by Eq. $R_{0i} = 1.28A_i^{1/3} - 0.76 + 0.8A_i^{-1/3}$.

2.4 Solution of the Schrödinger Equation and the fragments Preformation Probability (P_0)

Once the Hamiltonian in decoupled approximation Eq. (2.23) is established, the Schrödinger equation in mass fragmentation co-ordinate η can be solved.

$$H = \frac{-\hbar^2}{2\sqrt{B_{\eta\eta}}}\frac{\partial}{\partial_\eta}\frac{1}{\sqrt{B_{\eta\eta}}}\frac{\partial}{\partial_\eta} - \frac{\hbar^2}{2\sqrt{B_{RR}}}\frac{\partial}{\partial_R}\frac{1}{\sqrt{B_{RR}}}\frac{\partial}{\partial_R} + V(\eta) + V(R) \quad (2.23)$$

On solving Eq. (2.23) numerically, $|\psi^{v}(\eta)|^2$ gives the probability P_0 of finding the mass fragmentation η at a fixed R on the decay path.

$$P_0(A_2) = |\psi^{v}(A_2)|^2 \quad (2.24)$$

For fission studies, like the spontaneous fission and fission through the barrier, the motion in R at the saddle point is adiabatically slow as compared to the η motion. Therefore, the potential is minimized in the neck and deformation coordinates ß1 and ß2 at each R and η values. Starting from the nuclear ground state in spontaneous fission or cluster decay, and to have complete adiabaticity, only the lowest vibrational state $\nu = 0$ is occupied. Then, the mass (or charge) distribution yield, proportional to the probability $|\psi^{(0)}(\eta)|^2$ or $|\psi^{(0)}(\eta_z)|^2$ of finding a certain mass (or charge) fragmentation η (or η Z) at a position R on the decay path, when scaled to, say, mass A_2 of one of the fragments (d η =2/A) is given by:

$$Y(A_2) = |\psi_R^{(0)}(A_2)|^2 \frac{2}{A}\sqrt{B_{\eta\eta}(A_2)}). \quad (2.25)$$

However, if the system is excited or we allow interaction between various degrees of freedom, higher values of ν would also contribute. These enter via the excitation of higher vibrational states, and through the temperature dependent potential V and masses Bij .The effect of adding temperature on potential V and masses B_{ij} is to reduce the shell effects in them, resulting finally in the liquid drop potential VLDM and smoothed (averaged) masses Bij for the systems to be very hot.

Apparently, cold fission means taking both the potential V and masses Bij with full shell effects included in them and hot fission means using the VLDM and smoothed (averaged) masses Bij. The possible consequence of such excitations are included here by assuming a Boltzmann like occupation of excited states

$$|\psi(\eta)|^2 = \sum_{\nu=0}^{\infty} |\psi^{\nu}(\eta)|^2 \exp\left(-\frac{E_{\eta}^{\nu}}{T}\right) \tag{2.26}$$

We are dealing here with a directly measurable quantity, the mass (or charge) asymmetry, which works dynamically as mass (or charge) transfer coordinate. Thus, the calculated yields Y (Ai) (or Y (Zi)) are directly comparable with experiments. It may be stressed that there is no free parameter in these calculations. The nuclear shape, once minimized in the neck and deformation coordinates ß1 and ß2 at a given R (=Rsaddle), remains fixed for both the mass and charge distributions of fission or decay fragments.

2.5 Penetration Probability (P)

Penetrability P measures the capability of fragments nucleus to penetrate the potential barrier generalized during compound nucleus formation. The probability that a particle will pass through a potential barrier, that is, through a finite region in which the particle's potential energy is greater than its total energy is penetration probability.

2.6 Assault Frequency (υ_0)

For the cluster decay studies in the following section, another quantity of interest is the assault frequency υ_0 defined as,E_2

$$\upsilon_0 = \frac{\mathrm{v}}{\mathrm{R0}} = \frac{\sqrt{(2E_2/\mu)}}{\mathrm{R0}} \tag{2.27}$$

where R_0 is the radius of parent nucleus and E2 = $1/2\mu v^2$ is the kinetic energy of the emitted cluster. Since both the emitted cluster and the daughter nucleus are produced in the ground state, the entire positive Q-value is the total kinetic energy (Q = E1 + E2) available for the decay process, which is shared between two fragments, such that for the emitted cluster

$$E2 = \left(\frac{A1}{A}\right)Q \tag{2.28}$$

And, E1 = Q - E2 is the recoil energy of the daughter nucleus.

2.7 References

[1] R.K. Gupta, M. Balasubraniam, C. Mazzocchi, M. La Commara, and W. Scheid, Phys. Rev. C 65, 024601 (2002).

[2] M.K. Sharma, R.K. Gupta, and W. Scheid, J. Phys. G 26, L45 (2000).

[3] R.K. Gupta, R. Kumar, N.K. Dhiman, M. Balasubraniam, W. Scheid, and C. Beck, Phys. Rev. C 68, 014610 (2003).

[4] M. Balasubraniam, R. Kumar, R.K. Gupta, C. Beck, and W. Scheid, J. Phys. G 29, 2703 (2003): R.K. Gupta, M.K. Sharma and B. Singh, Phys. Rev. C-to be published

[5] R.K. Gupta, M. Balasubraniam, R. Kumar, D. Singh, and C. Beck, Nucl. Phys. A 738, 479c (2004).

[6] R.K. Gupta, M. Balasubramaniam, R. Kumar, D. Singh, C. Beck, and W. Greiner, Phys. Rev. C 71, 014601 (2005).

[7] B.B. Singh, M.K. Sharma, R.K. Gupta, and W.Greiner,Int.J. Mod.Phys.E15, 699 (2006)

[8] R.K. Gupta, M. Balasubraniam, R.Kumar, D.Singh ,S. K. Arun and W.Greiner,J.Phys .G:Nucl.Part. Phys. 32, 345(2006)

[9] B.B. Singh, M.K. Sharma, R.K. Gupta,Phys.Rev. C 77, 054613 (2008)

[10] R.Gupta, in proceedings of the 5th International Conference on Nuclear Research Mechanics, Varenna, 1988, edited by E. gladioli , (Ricerca Scientifica ed Educazione Permanente Milano, 1988),p.416.

[11] S.S. Malik and R.K.Gupta, Phys.Rev.C 39, 1992(1989)

[12] R.K.Gupta, W.Scheid, and W.Greiner, J.Phys.G:Nucl. Part. Phys. 17, 1731(1991).

[13] S. Kumar and R.K.Gupta, Phys.Rev. C 49, 1922(1994).

[14] R.K.Gupta and W. Greiner Int. J. Mod. Phys. E 3, 335 (1994, Suppl.).

[15] S. Kumar and R.K.Gupta, Phys. Rev. C 55, 218 (1997).

[16] R.K. Gupta, in Heavy Elements and Related New Phenomena ,edited by W.Greneir and R.K Gupta (World Scientific Singapore) Vol.II ,p.730

[17] S.K and R.K Gupta ,DAE nucl.Phys.(Sambalpur)52,365(2007)

[18] B.B.Singh, S.K Arun, M.K.Sharma , S.Kanwar and Raj K.Gupta ,DAE Nucl.Phys.(Roorkee), Accepted(2008)

[19] R.K. Gupta, N.Singh, and M. Manhas, Phys. Rev. C 70, 034608 (2004)

[20] R.K. Gupta ,M.balasubramaniam, R.Kumar, N.Singh, M.Manhas, and W. Greiner, J.Phjs. G: Nucl.Part. Phys. C 31, 631(2005).

[21] T. Matsuse, C. Beck, R. Nouicer, and D. Mahboub, Phys. Rev. C 55, 1380

(1997).

[22] S.J. Sanders, D.G. Kovar, B.B. Back, C. Beck, D.J. Henderson, R.V.F.

Janssens, T.F. Wang, and B.D. Wilkins, Phys. Rev. C 40, 2091 (1989t).

[23] S.J. Sanders, Phys. Rev. C 44, 2676 (1991).

[24] J. Gomez del Campo, R.L. Auble, J.R. Beene, M.L. Halbert, H.J. Kim, A.

D'Onofrio, and J.L. Charvet, Phys. Rev. C 43, 2689 (1991); Phys. Rev. Lett.

61, 290 (1988).

[25] R.J. Charity, M.A. McMahan, G.J. Wozniak, R.J. McDonald, L. G. Moretto,

D.G. Sarantites, L.G. Sobotka, G. Guarino, A. Pantaleo, L. Fiore, A. Gobbi

and K.D. Hildenbrand, Nucl. Phys. A 483, 371 (1988).

[26] C. Beck, R. Nouicer, D. Disdier, G. Duchˆene, G. de France, R.M. Freeman, F. Haas, A. Hachem, D. Mahboub, V. Rauch, M. Rousseau, S.J. Sanders, and A. Szanto de Toledo, Phys. Rev. C 63, 014607 (2001).

[27] N.J. Davidson, S.S. Hsiao, J. Markram, H.G. Miller, and Y. Tzeng, Nucl. Phys. A 570, 61c (1994).

[28] G. Audi and A.H. Wapstra, Nucl. Phys. A 595, 4 (1995).

[29] G. Audi and A.H. Wapstra and C. Thiboult, Nucl. Phys. A 729, 337(2003)

[30] P. M¨oller, J. R. Nix, W. D. Myers, and W. J. Swiatecki, At. Data Nucl. Data Tables 59, 185 (1995).

[31] W. Myers and W.J. Swiatecki, Nucl. Phys. 81, 1 (1966).

[32] P. A.Seeger, Nucl. Phys. 25, 1 (1961)

[33] H.Kroger and W. Scheid, J. Phys. G 6, L85(1980)

[34] S.J. Sanders, D.G. Kovar, B.B. Back, C. Beck, B.K. Dichter, D. Henderson, R.V.F. Janssens, J.G. Keller, S. Kaufman, T.-F. Wang, B. Wilkins, and F. Videbaek, Phys. Rev. Lett. 59, 2856 (1987).

CHAPTER-3

α- PARTICLE INDUCED FUSION-FISSION DYNAMICS

In view of present day developments in the domain of nuclear physics, it is extremely important & essential to study the nuclear behavior at the extreme conditions of temperature, angular momentum & energies in order to respond the exotic experimentations being conducted & planned in near future. In order to meet such challenges, it becomes extremely essential to update the standard of theoretical computations in order to make meaningful predictions in the related field. In the last six decades since the discovery of nuclear fission, extensive theoretical and experimental investigations have been carried out to understand the various aspects of fusion-fission dynamics.

The mass asymmetry factor is a useful parameter for different type of fission fragments observed in the decay of compound nucleus. The fission process in heavy elements has been studied with energetic probes such as photons, protons, and α-particle. The details of such experiments can be found in Ref [1] and [2].Beside this nuclear deformations and orientations seem to play prominent role in the formation as well as decay process of a nuclear system

Less is known about fission of lighter nuclei and the nuclear fission at higher energies where such nuclei can fission. If the angular momentum is high then the fission barrier is reduced and even light systems like ^{60}Zn can undergo fission [3]. Here we will concentrate on reactions induced by light charged particles and in particular α- particles. The low and medium mass region is interesting since it is predicted that for a fissility parameter Z^2 / A below 20, the system tends to become asymmetric. This is so called Businaro-Gallone point [4].

Nix and Sassi [5] found in calculations employing the liquid drop model that the probability for fission had a minimum at the quoted fissility parameter. Such a minimum corresponds of course to a maximum in the height of the fission barrier.

Alpha particle induced fission has been reported in [6] where α-particle is induced on ^{nat} Ag, ^{165}Ho, ^{139}La and ^{197}Au targets. The experiments were performed at the Juilich cyclotron. A beam of particles was focused onto the fissile targets in the centre of a scattering chamber which was 1 m in diameter. The beam was then dumped into a well shielded Faraday cup. The targets were ^{nat} Ag, ^{165}Ho, ^{139}La and ^{197}Au with thickness of 50 μg/cm^2 ,97 μg/cm^2 and 130 μg/cm^2 .The rare earth targets had backings of carbon with thickness of 30 μg/cm^2 (Ho).

Two different setups were used in the experiment [6]. In first, two solid state detectors of 30 mm diameter, cooled to -20 ^{0}, were mounted symmetrically left and right of the beam direction at angles corresponding to full momentum transfer to the compound nucleus. The solid angles were defined by collimator of 25 mm diameter. While the right detector was only 57 mm away from the target and the left one was at a distance of 150 mm. Thus if a fragment was detected in the smaller solid angle, its complementary fragment should always be detected in the larger solid angle. Coincidence circuits ensured that the two fragments were from the same reaction event. A high voltage of 10KV applied to the target holder prevented electrons from reaching the detectors.

The detectors were calibrated with fission fragments from a ^{252}Cf source applying the method of Schmitt et al [7] and Kaufmann et *al* [8].The calibrations were performed before the experiments and at regular intervals. The energies were calculated according to method given in Ref [8].The masses were estimated from $M_L=A_{CN}\ E_l/E_l+E_r$, with A_{CN} being the mass of the compound nucleus and similarly for M_r (right detector).

It is reported in [6] that while for the heavier targets it is rather simple to distinguish between fission fragments and background, this is not so for silver. For this target they have performed experiments with a different setup. Again to the right of the beam was solid state detector .To the left we employed ionization chamber, where the anode was subdivided to allow for ΔE-E measurements. Because of a Frisch grid, the signals were independent of the position of the ionization. Position measurements were performed using a proportional counter tube situated behind a slit in the anode. The position was calibrated with a movable slit between the ionization chamber and californium source. Energy calibration was performed as before, but corrections had to be applied for entrance window of the ionization chamber.

Backgrounds were eliminated by making cuts on the scatter plots of combinations of the following parameters: ΔE, time difference, position signal left and right of the proportional counter tube, and the energy signal in the solid state detector and in the ionization chamber.

The measured distributions of the total kinetic energies and the masses of the two fragments are depicted in [6]. In general the spectra have Gaussian shapes, as expected for high energy fission where shell effects are unimportant. The only exception is reported in the mass distribution in the case of silver target where the distribution shows more of a box-like form.

The measurements were analyzed assuming a fissioning system. These of course provide the most interesting information. However, the experiment records events after emission of particles

before the fragments have reached the detectors. The best choice for a necessary correction would have been through the measurement of the corresponding particle spectra, but this was not done in [6]. However a measurement of the correlation angle between the two fission fragments in the case of the gold target and found an almost complete linear momentum transfer from the projectile to the fissioning system similar to that in Ref. [9]. The results are obtained for mean

Momentum carried away near the forward direction by protons and neutrons during the pre-equilibrium phase by making use of the exciton model with standard input parameters [10]. In the case of the gold target, neutrons are shown to carry away ≈255 MeV/c but with 0.22 neutrons per incident α particle. For protons, the mean momentum is higher, ≈285 MeV/c, but the rate is only 0.14 protons per α particle.

In [6] an attempt is made to fill a gap between these lower energy data and results at higher energies [11]. It is worth noting that the cross section in the case of the silver target comes out to be smallest.

The only data for 140 MeV α particle are for bismuth and uranium [12]. The fission probability for bismuth is almost an order of magnitude larger than that for gold and for uranium it is about unity. Since no data exist for particle induced fission for lower masses, the authors of [6] present data with those from proton-induced reactions at energies close by. There is a remarkable agreement between the results for the two entrance channels. While the two methods give similar results in case of the gold target they diverge more for the lighter systems.

Fission of four nuclei such as silver, lanthanum, holmium and gold induced by 140 MeV α particles reported in [6] is studied within Dynamical cluster decay model (DCM) approach in order to look for mass fragmentation path and related aspects for an alpha particle induced fission process.

RESULTS AND DISCUSSIONS

Fig. 3.1 shows the fragmentation potential as a function of fragment mass for α-induced fission of ^{nat} Ag target. The fragments in the range of 32-44 seem to contribute towards fission (asymmetric) fragments. The interesting aspect of the study is that α–nucleus structure is quite prominent even at energy as higher as 140 MeV.

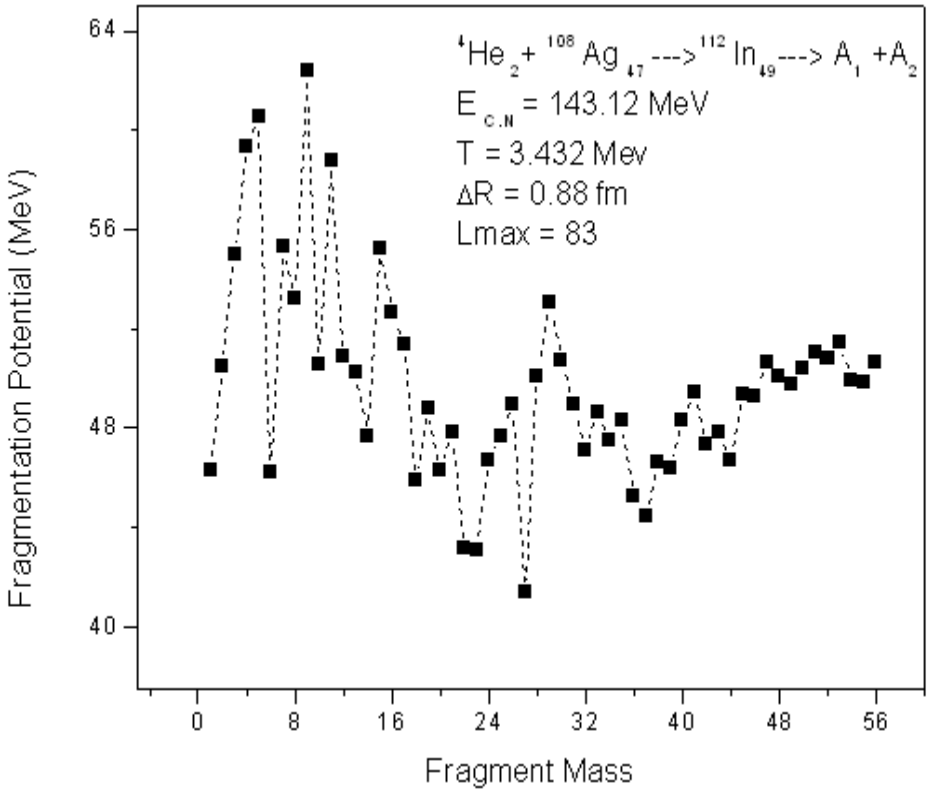

Fig. 3.1 Fragmentation potential as a function of fragment mass for ^{Nat} Ag

Fig. 3.2 shows the fragmentation potential as a function of fragment mass for α-induced fission of ^{139} La target. The fragments in the range of 52 - 57 and 69 - 73 (see fig. 3.6) seem to contribute towards fission (asymmetric) fragments. The interesting aspect of the study is that α–nucleon structure is quite prominent for fragment mass less than 31 even at energy as higher as 140 MeV. The dips across ^{18} O and ^{27} Al should not be taken seriously as the prominence of these fragments get ruled out by a very small penetrability of these fragments as discussed in fig.3.10, which gives penetration probability for this reaction.

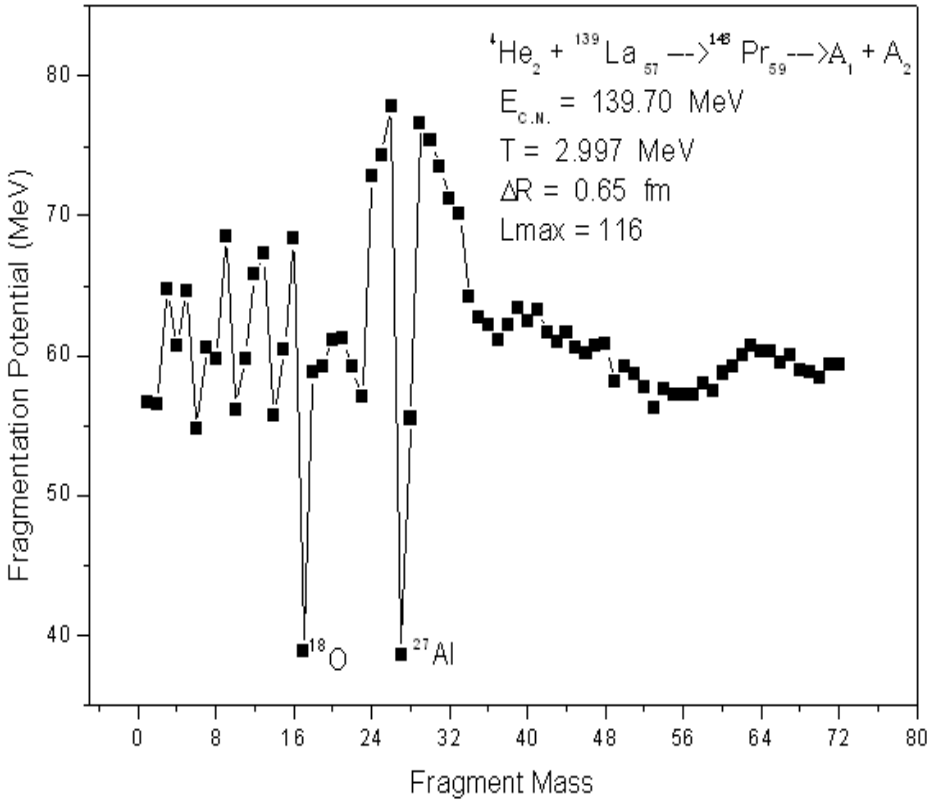

Fig. 3.2 Fragmentation potential as a function of fragment mass for ^{139} La

Fig. 3.3 shows the fragmentation potential as a function of fragment mass for α-induced fission of ^{165} Ho target. The fragments in the range of 30 - 40 seem to contribute towards fission (asymmetric) fragments. The interesting aspect of the study is that α–nucleon structure is quite prominent for fragment mass less than 40 even at energy as higher as 140 MeV. The dips across ^{18} O and ^{27} Al should not be taken seriously as the prominence of these fragments get ruled out by a very small penetrability of these fragments as discussed in fig. 3. 11

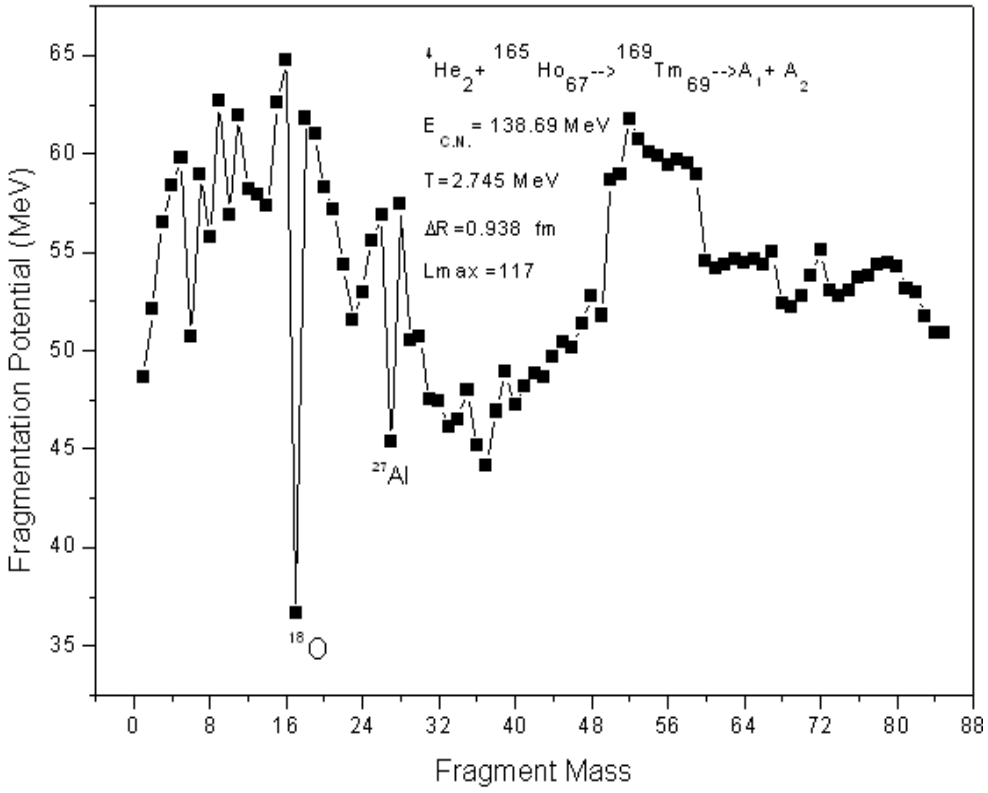

Fig. 3.3 Fragmentation potential as a function of fragment mass for ^{165} Ho

Fig. 3.4 shows the fragmentation potential as a function of fragment mass for α-induced fission of ^{197} Au target. The fragments in the range of 62-78 and 97-104 seem to contribute towards fission (asymmetric) fragments. The dips across ^{18} O and ^{27} Al should not be taken seriously as the prominence of these fragments get ruled out by a very small penetrability of these fragments in fig. 3.12 .The interesting aspect of the study is that α–nucleon structure is not so prominent as that for other cases under investigation at E=140 MeV.

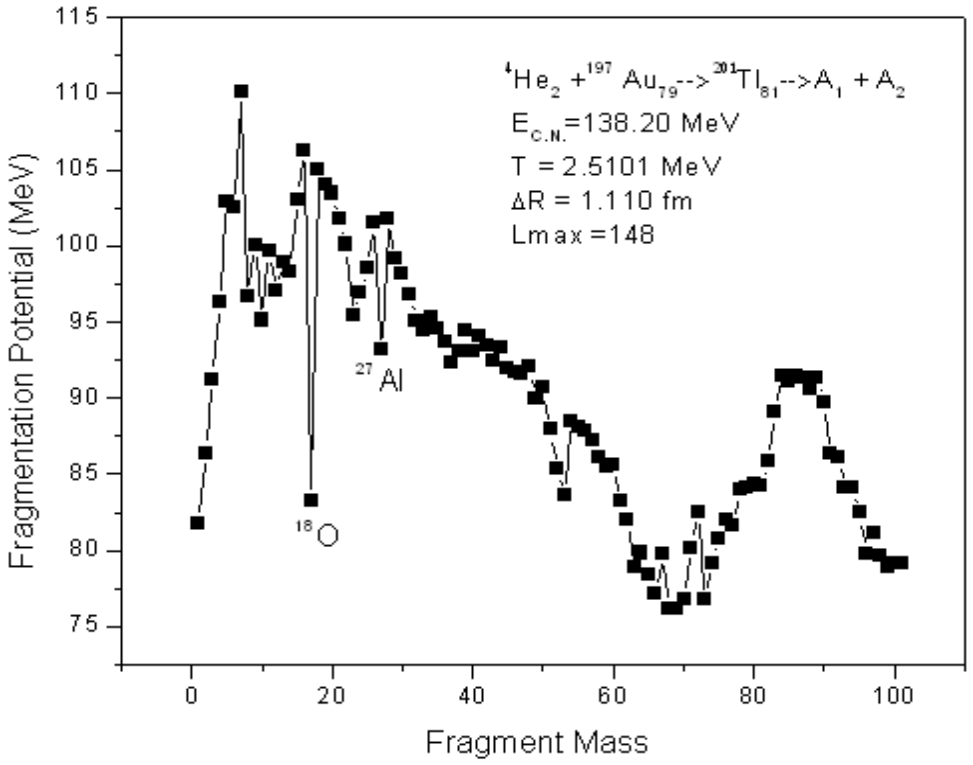

Fig. 3.4 Fragmentation potential as a function of fragment mass for ^{197} Au

Fig. 3.5 shows the preformation probability of alpha particle induced fission of ^{nat}Ag target. The fragments in the mass region 32-44 contribute for fission fragments. It is relevant to mention here that preformation probability is an important parameter within DCM approach and it carries the much required information regarding nuclear structure and related aspects. This parameter gives an account of probability of formation of decaying fragments at the compound nucleus state. Interestingly the DCM preformation probability gives a box kind of behavior as reported in the lower most panel of Fig. 2 of [6].

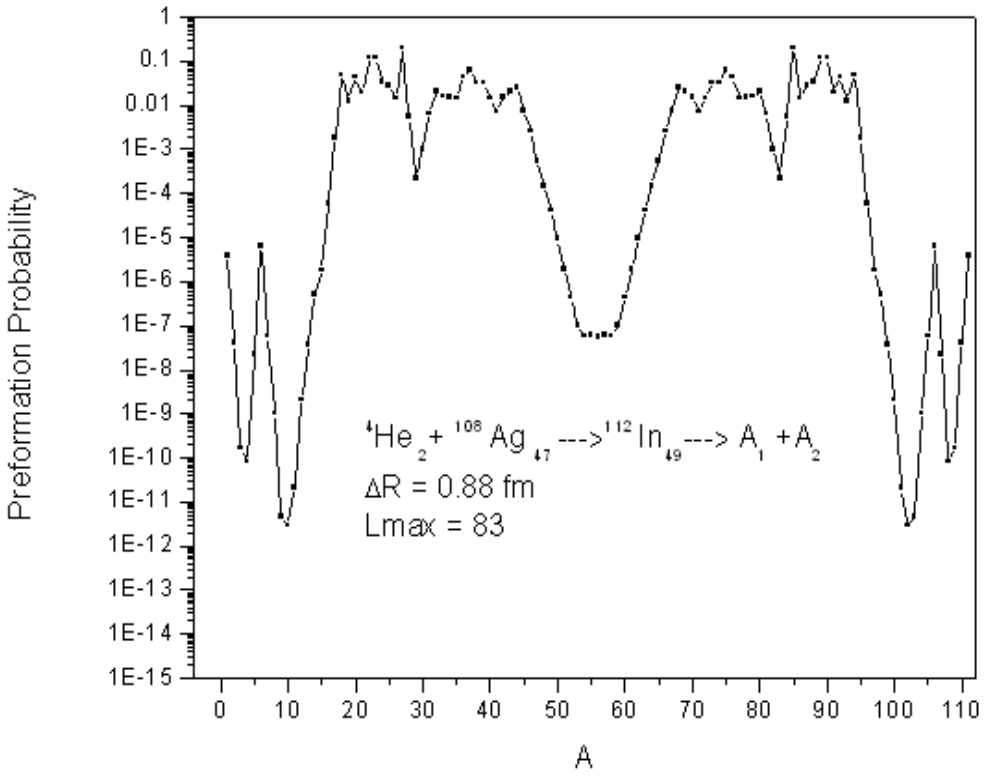

Fig. 3.5 Preformation probability as a function of fragment mass for ^{nat}Ag

Fig. 3.6 shows the preformation probability of alpha particle induced fission of ^{139}La target. The fragments in the mass region 52-57 and 69-73 seem to contribute for fission fragments. Preformation probability provides information regarding nuclear structure which is important parameter to study fission dynamics. In fig. 3.6 it is clearly evident that in the α-induced fission of La target mass ranges 40-100 is almost Gaussian as reported in second lower panel of fig. 2 of [6].However cluster like structure is seen in the decay of this nuclear system and the cluster in the range of masses 15-30 seem very prominent. It will be of interest to look out the penetrability of these fragments before reaching at any conclusion.

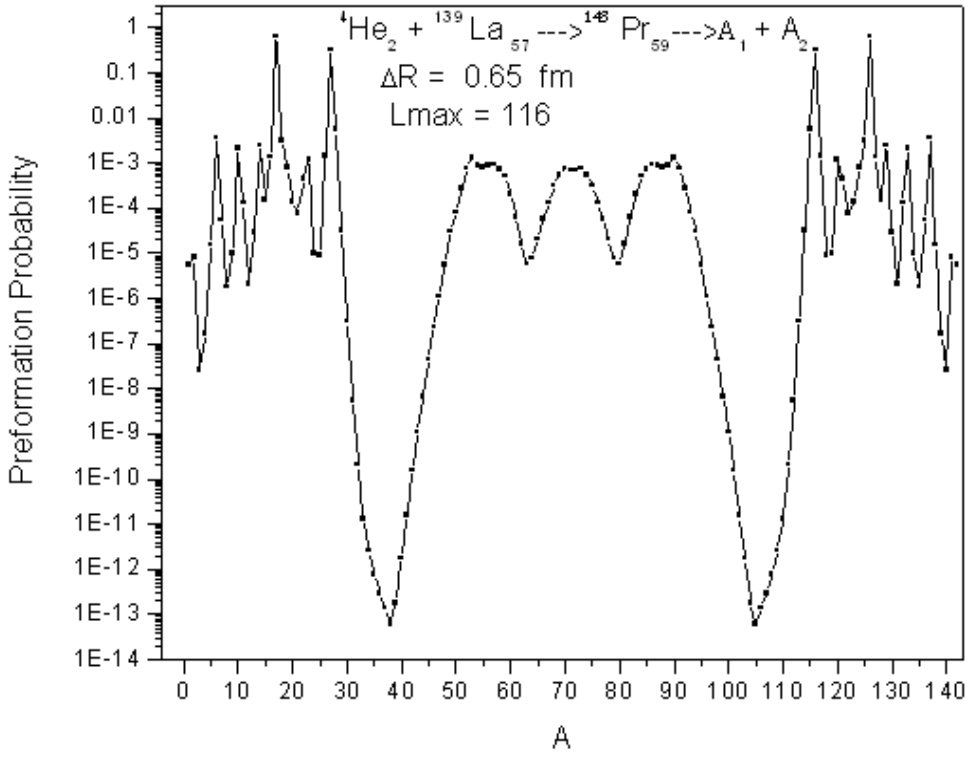

Fig. 3.6 Preformation probability as a function of fragment mass for ^{139}La

Fig. 3.7 shows the preformation probability of alpha particle induced fission on ^{165}Ho target. Preformation probability gives information about the probability of formation of fragments as compound nucleus decays. Prominence for cluster formation is also observed in the α-induced decay of Ho as reported in fig. 3.7 and some clusters/fragments in the mass range 30-40 seem to be contributing towards probable cross-sections. The fragments with mass less than 30 get ruled out due to their small penetration probability reported in fig. 3.11.

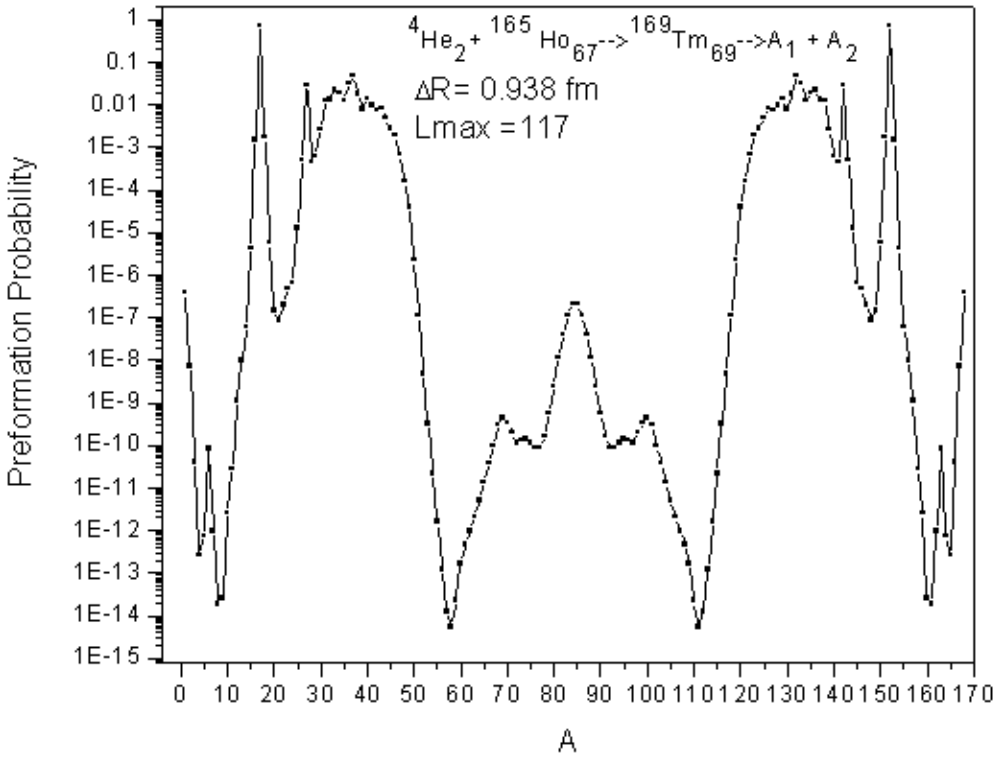

Fig. 3.7 Preformation probability as a function of fragment mass for ^{165}Ho

Fig. 3.8 shows the preformation probability of alpha particle induced fission of ^{197}Au target. The fragments in the mass range 62 - 78 and 97 - 104 contribute for fission fragments. It provides information about the preformation probability of decaying system, ^{201}Tl.

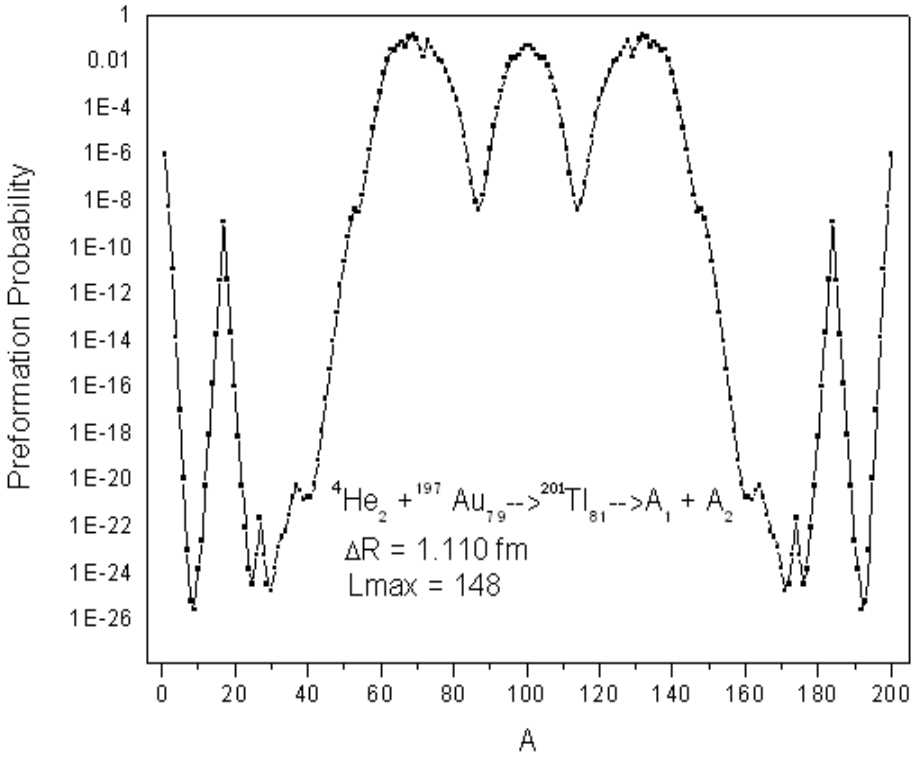

Fig. 3.8 Preformation probability as a function of fragment mass for ^{197}Au

Fig. 3.9 shows the WKB Penetrability for α-induced fission of ^{nat}Ag. It is relevant to mention here that penetrability contributes mainly in the magnitude and play a salient role in regard to structure and related aspects. As the penetrability for fragments A_2 = 15-30 is quite small for silver target, the reaction under investigation. It is important to recall that the fragment formation probability of ^{18}O and ^{27}Al was quite high but the same gets ruled out by extremely small penetrability of these fragments in the decay of ^{112}In.

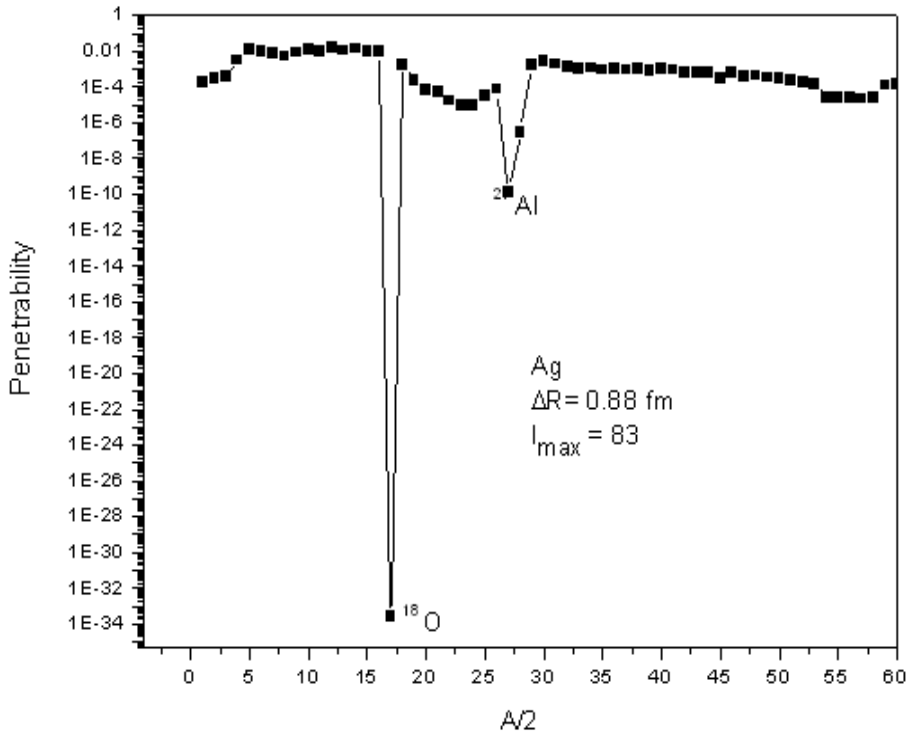

Fig. 3.9 WKB Penetrability for α-induced fission of ^{nat}Ag

Fig.3.10 shows the WKB Penetrability for α-induced fission of ^{139}La target. The penetrability for fragments in the range 15-30 is again quite small, so the prominent clusters emerged in case La target get suppressed via relatively weaker penetration probabilities. WKB method is applicable whenever the potential is slowly varying. As fragment formation probability of ^{18}O and ^{27}Al was quite high but they have extremely small penetrability in the decay of ^{143}Pr.

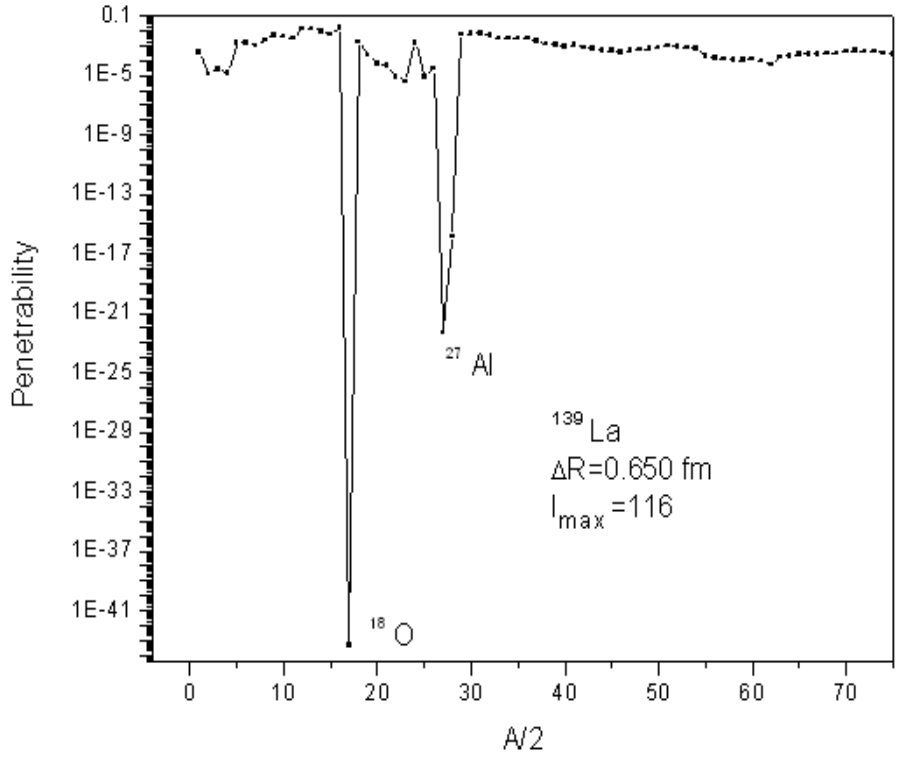

Fig. 3.10 WKB Penetrability for α-induced fission of ^{139}La

Fig. 3.11 shows the WKB Penetrability for α particle induced fission of ^{165}Ho target. It provides information about the extent up to which fragments can penetrate. It is clear from the graph that the penetration probability for Oxygen and Aluminum is very small as compared to other fragments.

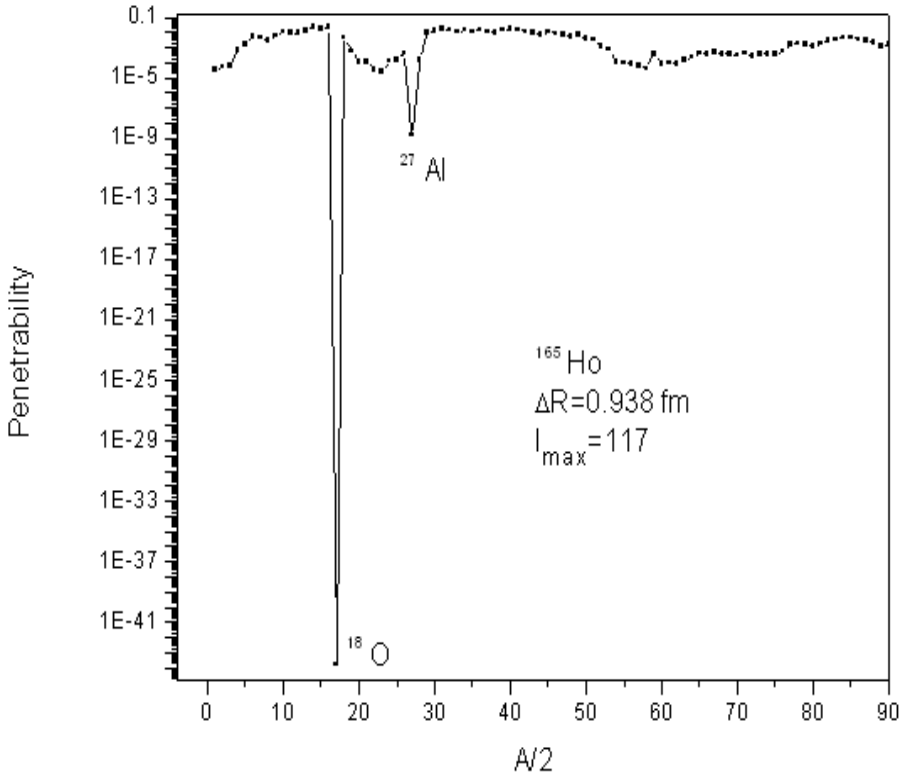

Fig. 3.11 WKB Penetrability for α-induced fission of ^{165}Ho

Fig. 3.12 shows the WKB Penetrability for α-induced fission of ^{197} Au target. Again the penetrability contributes mainly in the magnitude and plays a salient role in regard to structure. Here the penetration probability of fragments in range 15 – 30 is quite small.

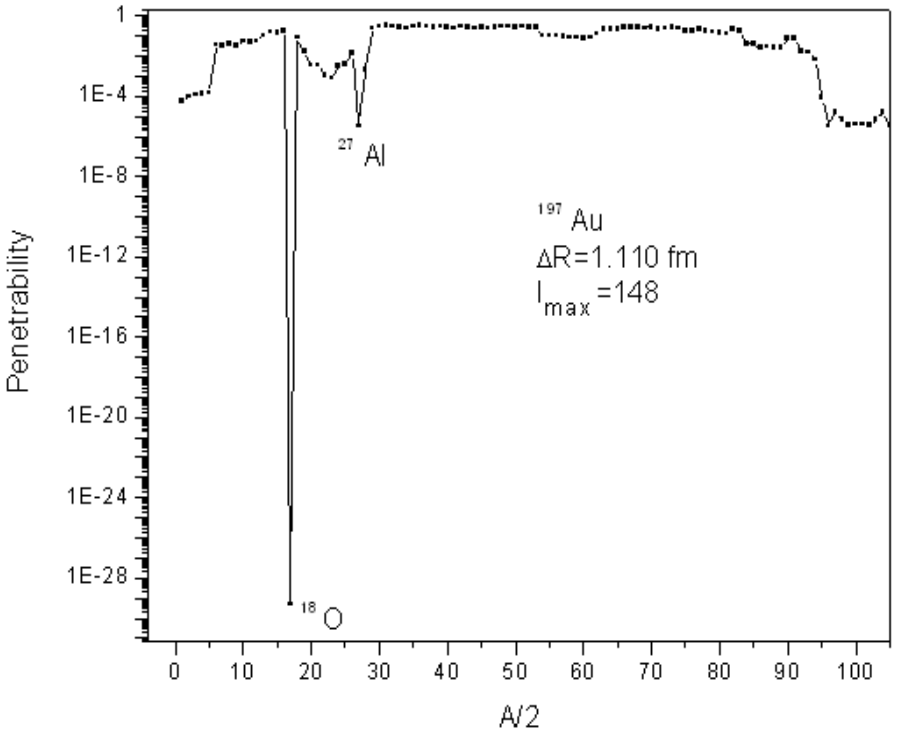

Fig. 3.12 WKB Penetrability for α-induced fission of ^{197} Au

Table 3.1 shows the comparison of DCM results along with other related DCM parameters.

Sr. No.	Projectile	Target	CN	$E_{C.N.}$ (MeV)	ΔR (fm)	Temp.	l_{max}	DCM $\sigma_{fission}$ (mb)	Expt. $\sigma_{fission}$ (mb)
1.	α- particle	^{nat}Ag	^{112}In	143.12	0.880	3.432	83	0.046	0.030±0.007
2.	α- particle	^{139}La	^{143}Pr	139.70	0.650	2.997	116	0.0003	0.007±0.001
3.	α- particle	^{165}Ho	^{169}Tm	138.69	0.938	2.745	117	0.820	0.600±0.050
4.	α- particle	^{197}Au	^{201}Tl	138.20	1.110	2.5101	148	105.0	128±18

The comparative data for ^{nat}Ag, ^{165}Ho and ^{197}Au target is given in table1. The DCM results find reasonable comparison with experimental data although there is a definite scope of improvement as far as present set of calculations is concerned. Interestingly ΔR and l_{max} seem to increase with increase in target mass except for ΔR in case of ^{139}La target. It may be recalled that cluster kind of behavior is seen in case of thin target and measured cross-sections are quite small.

REFERENCES

[1] R. Vandenboosch and J. R. Huizenga, Nuclear Fission (Academic Press, New York/ London 1973).

[2] C. Wagemans, The Nuclear Fission Process (CRC Press, Boca Raton, 1991).

[3] W.von Oertzen et al., Phys. Rev. C **78**, 044615 (2008).

[4] U. L. Businaro and S. Gallone, Nuovo Cimento 5, 315 (1957).

[5] J. R. Nix and E. Sassi, Nucl. Phys. **81**, 61 (1966).

[6] A.Buttkewitz, H.H.Duhm, F. Goldenbaum, H. Machner and W. StrauB Phys. Rev. C **80**,037603 (2009)

[7] H. W. Schmitt, W. E. Kiker, and C. W. Williams, Phys. Rev. **137,** B837 (1965).

[8] B. Kaufmann et al., Nucl. Instrum. Methods **115**, 47 (1974).

[9] V. E. Viola, C. T. Roche, W. G. Meyer, and R. G. Clark, Phys. Rev. C **10**, 2416 (1974).

[10] H. Machner, Phys. Rep. **127**, 309 (1985).

[11] G. Klotz-Engmann et al., Nucl. Phys. A **499**, 392 (1989).

[12] W. G. Meyer, V. E. Viola, R. G. Clark, S. M. Read, and R. B. Theus, Phys. Rev. C **20**, 1716 (1979).